

The asymmetry of recirculation of a double gyre in a two layer ocean

Shinya Shimokawa (下川信也)*

Tomonori Matsuura (松浦知徳)*

*National Research Institute for Earth Science and Disaster Prevention (防災科学技術研究所),
Tennodai 3-1 Tsukuba, Ibaraki, 305-0006, Japan

1 Introduction

Holland (1978) showed that, in the modeling of a double gyre using a two layer quasi-geostrophic (QG) model, a symmetric wind forcing produces a symmetric circulation pattern. In this situation, the subpolar gyre is merely a mirror image of the subtropical gyre.

However, it is well known that the QG model ignores the nonlinearity associated with layer thickness change and is only valid in the case where the layer thickness change is much smaller than the undisturbed layer thickness. In the case where the nonlinearity with the layer thickness is large, the QG model can not describe the realistic pattern of the ocean general circulation. By using non-QG models which include the nonlinearity with layer thickness, many studies showed that a symmetric wind forcing produces an asymmetric circulation pattern (Huang, 1986, Chassignet & Gent, 1991, Chassignet, 1992, Chassignet & Bleck, 1993) and the cyclonic vortex splits into meso-scale vortices more easily than the anti-cyclonic vortex when the

vertical displacement is large (Cushman-Roisin et al., 1992, Tang & Cushman-Roisin, 1992, Matsuura, 1995, Arai, 1994).

The main purpose of our study is to investigate the asymmetry of the recirculation of the double gyre, especially the asymmetry of the activities of the eddies using an eddy-resolving two layer primitive-equation model forced by symmetric wind stress.

2 Model

The basic equations are the same as for the two layer primitive-equation model used in Holland & Lin (1975). The model domain is 2560 km in both width and length, while the horizontal resolution is 20 km. The rotation parameters are taken as $f_0 = 7.3 \times 10^{-5} \text{ s}^{-1}$ and $\beta = 2.0 \times 10^{-11} \text{ m}^{-1} \text{ s}^{-1}$. The reduced gravity is $g^* = 2.0 \times 10^{-2} \text{ m s}^{-2}$. A non-slip boundary condition is imposed at the sidewalls. The wind stress, τ , is symmetric about the center of the model domain as follows:

$$\tau(y) = -\tau_0 \cos\left(\frac{2\pi y}{L}\right)$$

where $\tau_0 = 0.1 \text{ N m}^{-2}$, $L = 2560 \text{ km}$, y is the distance from the south edge of the model domain. The north region of the model domain represents the subpolar gyre, while the south region of it represents the subtropical gyre. Initial values of the velocities are zero. The integration is carried out for 5000 days.

We performed four experiments. Case 1 is the case with a 2000m upper layer thickness (H_1), 3000m lower layer thickness (H_2) and $3.3 \times 10^2 \text{ m}^2 \text{ s}^{-1}$ lateral viscosity (Ah). Case 2 is the case with $H_1=1000\text{m}$, $H_2=4000\text{m}$ and $Ah=3.3 \times 10^2 \text{ m}^2 \text{ s}^{-1}$. Case 2l is the case with $H_1=1000\text{m}$,

$H_2=4000\text{m}$ and $Ah=1.0 \times 10^2 \text{ m}^2\text{s}^{-1}$. Case 3 is the case with $H_1=500\text{m}$, $H_2=4500\text{m}$ and $Ah=3.3 \times 10^2 \text{ m}^2\text{s}^{-1}$.

3 Results

(a) The effect of layer thickness

We investigate the effect of the nonlinearity with the layer thickness on the asymmetry of recirculation of the double gyre in this section. Figure 1 (a), (b), (c) shows the layer thickness change (η) at day 1500 for (a) Case 1, (b) Case 2, (c) Case 3. When the upper layer is thick (Case 1), η becomes small and when the upper layer is thin (Case 3), η becomes large. The small η for Case 1 implies that there is no unsteady vortex in either the subpolar gyre or the subtropical gyre. That is, both the subpolar gyre and the subtropical gyre have laminar flow pattern and the circulation is nearly symmetric. For Case 2, although the recirculation of the subtropical gyre does not split, the recirculation of the subpolar gyre splits into many small vortices. That is, although the subtropical gyre has a laminar flow pattern, the subpolar gyre has a turbulent flow pattern and the circulation is asymmetric. For Case 3, η is large and, therefore, there are many vortices in both the subpolar gyre and the subtropical gyre. In other words, both the subpolar gyre and the subtropical gyre have a turbulent flow pattern. Therefore, from the view of the activities of the eddies, the asymmetry of recirculation of the double gyre is not noticeable. In this case, there are mainly three unstable areas: the recirculations of the double gyre, the return flow of the subpolar gyre and the mid-latitude jet.

(b) Lower viscosity case

In this subsection, we will investigate the Case 21 experiment. The viscosity for Case 21 is lower than that for Case 2. Figure 2 shows the upper layer pressure (P_1), the lower layer pressure (P_2), the layer thickness change (η) and the stream function (ψ) averaged over days 2000-2500 for Case 21. P_1 shows that the surface circulation consists of asymmetric twin gyres with western boundary currents, a eastward mid-latitude jet, asymmetric inertial recirculations near the jet and broad Sverdrup return flows. Although both the subpolar gyre and the subtropical gyre have a turbulent flow pattern (cf. Fig.4, stated in detail later), the asymmetry of recirculation of the double gyre for Case 21 is noticeable in spite of the magnitude of lateral viscosity. We can see that the recirculation of the subpolar gyre is stronger than that of the subtropical gyre. Especially, the difference of P_2 between the subpolar gyre and the subtropical gyre is noticeable. That is, the recirculation of the subpolar gyre is more barotropic than the recirculation of the subtropical gyre (cf. Fig.2(c), (d)). The recirculation of the subpolar gyre is more unstable and filled with more vortices than that of the subtropical gyre (cf. Fig.4). Therefore, the momentum transmission from the upper layer to the lower layer through the interfacial form drag in the subpolar gyre is more intensive than that in the subtropical gyre. This is the reason why the recirculation of the subpolar gyre is more barotropic than that of the subtropical gyre.

Next, we show how and where meso-scale eddies are mainly generated for Case 21. Figure 3 shows the time series of the basin-averaged energies for Case 21. The energy conversion occurs between the available potential energy (ap) and the total kinetic energy (tk): for

example, the conversion from tk to ap ($tk \rightarrow ap$) at days 2300 and 2600 (shown by arrows a and c, respectively) and the conversion from ap to tk ($ap \rightarrow tk$) at days 2400 and 2900 (shown by arrows b and d, respectively). We can expect that when $ap \rightarrow tk$, many eddies can be generated due to the instabilities, on the other hand, when $tk \rightarrow ap$, the circulation is considerably stable. Figure 4 and 5 show the upper layer pressure (P_1) and the lower layer pressure (P_2), respectively, at days 2300, 2400, 2600, and 2900 for Case 21. At days 2300, 2600, there is a large recirculation in the upper layer, especially on the subtropical side and there is a weak Rossby eddy pattern in the lower layer. At day 2400, the recirculation splits some vortices and the Rossby eddies are generated intensively in the lower layer, especially on the subpolar side. At day 2900, the mid-latitude jet meanders and the Rossby waves appear symmetrically in the lower layer. Holland et al.(1984) stated that in the QG model, the eddy field arises due to a combined baroclinic/barotropic instability of the eastward jet, baroclinic instability of the tight westward recirculation, and baroclinic instability of the distant westward return flow. We can consider that the case at day 2400 is a typical example of the instability of the recirculation and the case at day 2900 is that of the mid-latitude jet.

4 Summary and discussion

We obtained the following results:

- (1) The cyclonic recirculation becomes unstable and splits into meso-scale vortices more easily than the anti-cyclonic recirculation. Therefore, the subpolar gyre is filled with more vortices than the subtropical gyre.
- (2) The asymmetry of the recirculation of the double gyre is noticeable

in the case with realistic physical parameters from the view of the activities of the eddies. The recirculation of the subpolar gyre is stronger and more barotropic than that of the subtropical gyre.

Results (1) and (2) can be related to the fact that the subtropical gyre is well defined, but the subpolar gyre is not clearly defined in the North Pacific (e.g. Nagata et al., 1992). Our results suggest that in the North Pacific, the subpolar gyre is filled with more vortices than the subtropical gyre. Moreover, it is known that almost all of the large scale long-lived vortices on Jupiter and Saturn are anti-cyclones (e.g. Nezlin & Snezhkin, 1993). This can be also related to result (1) because the nonlinearity of the continuity equation can not be neglected for Jupiter's atmosphere (Williams & Yamagata, 1984).

References

- Arai, M (1994): Ph.D. thesis, Kyusyu Univ., pp.101.
- Chassignet, E.P.(1992): *J.Geophys.Res.*, **97**, 9479-9492
- Chassignet, E.P. and P.R.Gent (1991): *J.Phys.Oceanogr*, **21**, 1290-1299
- Chassignet, E.P. and R.Bleck (1993): *J.Phys.Oceanogr*, **23**, 1485-1507
- Cushman-Roisin, B. , G.G.Sutyrin, B.Tang (1992): *J.Phys.Oceanogr.*, **22**, 117-127
- Holland, W.R. and L.B.Lin (1975): *J.Phys.Oceanogr.*, **5**, 642-657
- Holland, W.R., T.Keffer and P.B.Rhines (1984): *Nature*, **308**, 698-705
- Huang, R.X. (1986): *J.Phys.Oceanogr.*, **16**, 1636-1650
- Matsuura, T. (1995): *J.Phys.Oceanogr.*, **25**, 2298-2318
- Nagata, Y., K.Ohtani and M.Kashiwai (1992): *Umi no Kenkyu*, **1**, 75-104.
- Nezlin, M.V. and E.N.Snezhkin (1993): *Rosby vortices, spiral structures, solitons*, Springer-Verlag, pp225
- Tang, B. and B.Cushman-Roisin(1992): *J.Phys.Oceanogr.*, **22**, 128-138
- Williams,G.P. and T.Yamagata (1984): *J.Atmos.Sci.*, **15**, 453-478

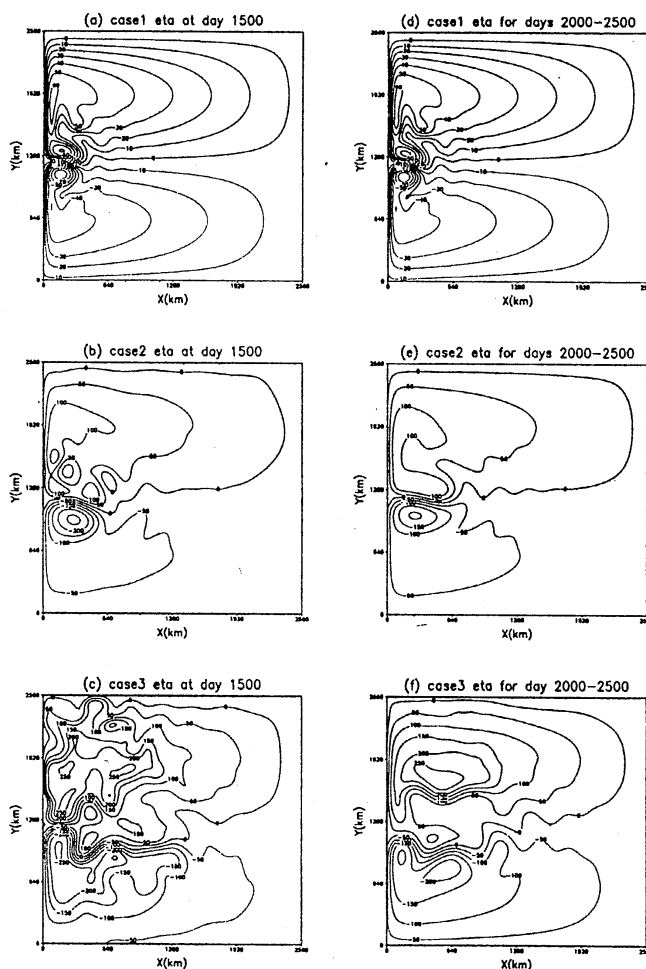


Fig.1 Layer thickness change at day 1500 for (a) Case 1 (CI=10 m), (b) Case 2 (CI=50m), (c) Case 3 (CI=50m) and averaged over days 2000-2500 for (d) Case 1 (CI=10m), (e) Case 2 (CI=50m), (f) Case 3 (CI=50m).

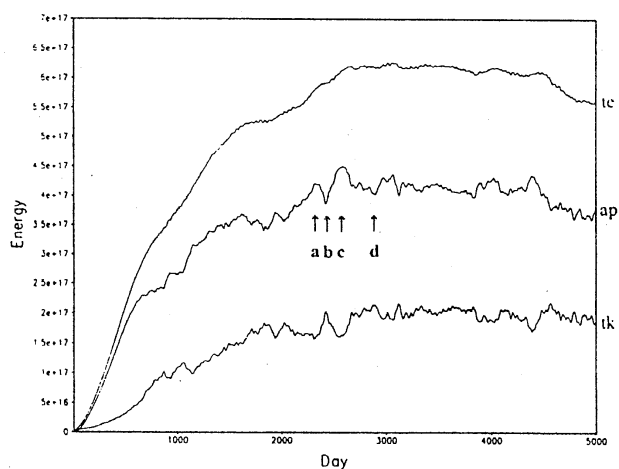


Fig.2 Time series of basin averaged energies for Case 2l. t_e ($=ap+tk$), ap ($=\iint 0.5 \Delta \rho g (\Delta h)^2 dS$), tk ($=\iint 0.5 \rho h_1 (u_1^2 + v_1^2) dS + \iint 0.5 \rho h_2 (u_2^2 + v_2^2) dS$) represent total energy, available potential energy, total kinetic energy, respectively. The unit is $kg m^2 s^{-2}$. The arrows show the positions where the rapid conversions between ap and tk occur (See the text).

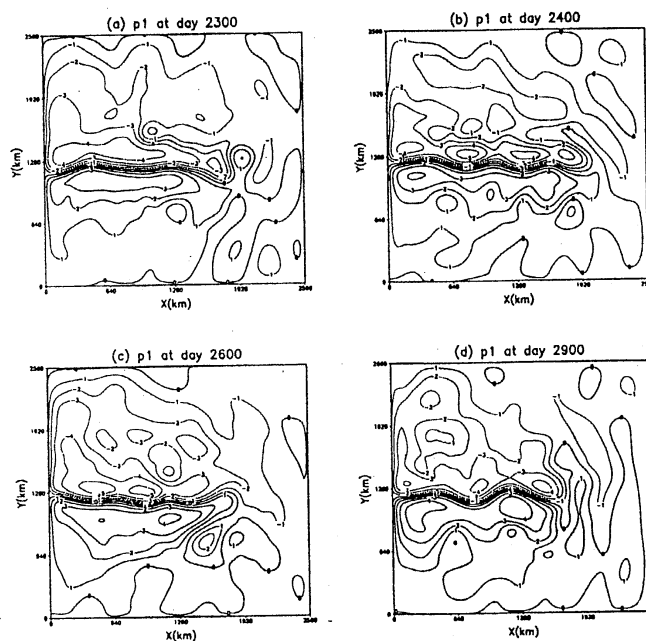


Fig.3 Upper layer pressure ($p1: CI = 1.0 \text{ m}^2 \text{ s}^{-2}$) at (a) day 2300, (b) day 2400, (c) day 2600, (d) day 2900 for Case 21.

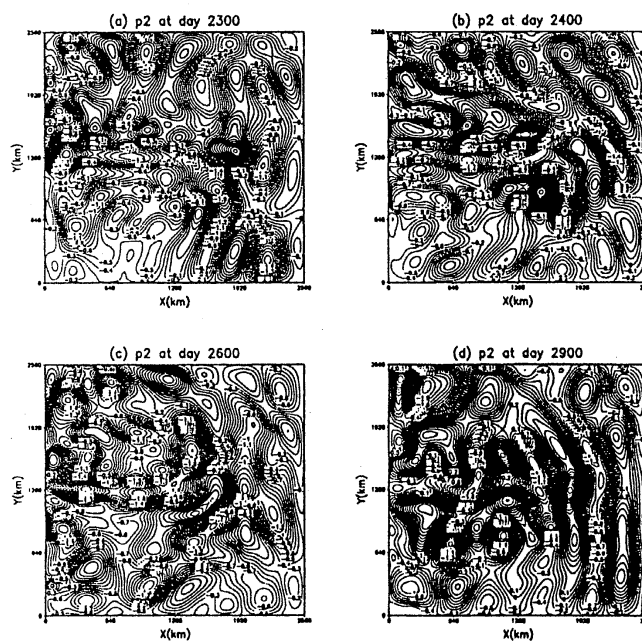


Fig.4 Lower layer pressure ($p2: CI = 0.1 \text{ m}^2 \text{ s}^{-2}$) at (a) day 2300, (b) day 2400, (c) day 2600, (d) day 2900 for Case 21.